New Grain Formation during Warm Deformation of Ferritic Stainless Steel

ANDREY BELYAKOV, RUSTAM KAIBYSHEV, and TAKU SAKAI

Microstructural evolution accompanied by localization of plastic flow was studied in compression of a ferritic stainless steel with high stacking fault energy (SFE) at 873 K (≈0.5 *Tm*). The structure evolution is characterized by the formation of dense dislocation walls at low strains and subsequently of microbands and their clusters at moderate strains, followed by the evolution of fragmented structure inside the clusters of microbands at high strains. The misorientations of the fragmented boundaries and the fraction of high-angle grain boundaries increase substantially with increasing strain. Finally, further straining leads to the formation of new fine grains with high-angle boundaries, which become more equiaxed than the previous fragmented structure. The mechanisms operating during such structure changes are discussed in detail.

I. INTRODUCTION

HOT deformation of various metallic materials with low to moderate stacking fault energy (SFE) leads to the evolution of new grain structure, that is, the occurrence of discontinuous dynamic recrystallization (DRX). Its fundamental features, such as plastic flow behaviors and the evolution of DRX grains and their substructures, have been studied in detail.[1,2,3] On the other hand, the evolution of new grains with high-angle boundaries sometimes takes place in higher SFE materials even during cold or warm deformation.[4–7] In this case, the structural changes do not result from DRX and are usually associated with the appearance of high-angle dislocation boundaries, such as microbands or shear bands, which are accompanied with a decrease in the strain hardening.[8–14]

There is a limited amount of work on the microstructure evolution of bcc metals during deformation at ambient to moderate temperatures.[4,7–9] Dimek and Blicharski[9] studied the structural changes of a ferritic steel with deformation at ambient temperature and found that the substructures composed of dislocation-rich layers, *i.e.*, the dense dislocation walls (DDWs), were formed in homogeneous cellular structures at an early stage of deformation, and microbands were developed in the initial grain interiors with further straining. Rybin *et al.*[8] originally termed such structures, including microbands and DDWs, the fragmented structure.

The aim of the present work is to study the changes in heterogeneous microstructures with deformation at moderate temperatures and particularly the dynamic processes of new fine grain evolution taking place in a ferritic steel with high SFE. The characteristics of heterogeneous dislocation substructures and the mechanisms operating during such dynamic processes are discussed in detail.

ANDREY BELYAKOV, Research Associate, and TAKU SAKAI, Professor, are with the Department of Mechanical and Control Engineering, the University of Electro-Communications, Chofu, Tokyo 182, Japan. RUSTAM KAIBYSHEV, Professor, is with the Institute for Metals Superplasticity Problems, Khalturina 39, Ufa 450001, Russia.

II. EXPERIMENTAL PROCEDURE

The material tested was a hot-rolled ferritic stainless steel, having the following chemical compositions: C0.13, Cr25, Ti0.9, and balance Fe (all in mass pct). Specimens 10 mm in diameter and 12 mm in height were machined parallel to the rolling direction and then annealed at 1523 K for 1 hour, leading to the evolution of an average grain size of 250 μm. Compression tests with no lubricant were conducted at 873 K (0.5 *Tm*) under strain rates of 10^{-4} to 10^{-2} s^{-1} using Instron 1185 and Schenck RMS-100 universal testing machines. For the observation of deformed structures, the specimens tested were quenched by water jet immediately after warm deformation. Some specimens were cut and polished parallel to the compression axis before testing and were then compressed for the observation of deformation relief. The slip patterns were studied with a JSM-840 scanning electron microscope. The metallographic observations were carried out in a Neophot-2 optical microscope and an Epiquant automatic structure analyzer. The dislocation substructures were examined in a JEM-2000EX transmission electron microscope (TEM), and misorientations were determined by a Kikuchi-line technique. X-ray analyses were also performed by Bragg–Brentano focusing.

III. RESULTS

A. *Deformation Behavior*

A series of true stress–true strain ($\sigma - \varepsilon$) curves for the present ferritic steel is depicted in Figure 1. Their general shapes are similar to those controlled only by dynamic recovery.[3] It can be seen clearly that flow stresses in each curve approach a saturation value at strains of around 0.25. The saturation stresses at high strains show relatively low strain rate dependence. This suggests that strain hardening and dynamic softening establish an equilibrium, and the deformation mechanisms operating do not change at high strains. Heterogeneous deformation, however, frequently took place at high strains in the present test conditions, as described later, and so this steady-state flow represents only an average macroscopic response to strain.

Figure 2 demonstrates the relationships between the steady-state flow stress (σ_{ss}) and strain rate ($\dot{\varepsilon}$) at 873 K.

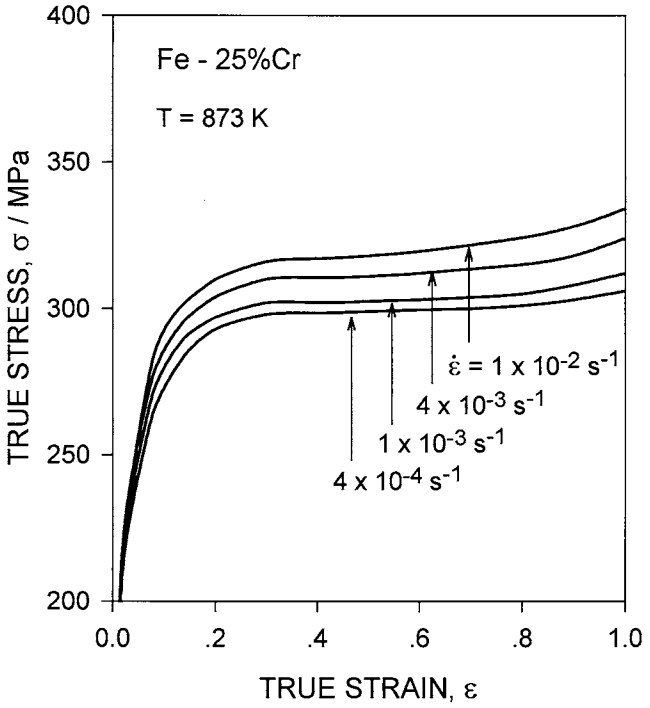

Fig. 1—A series of true stress–true strain curves for Fe-25 pct Cr at 873 K.

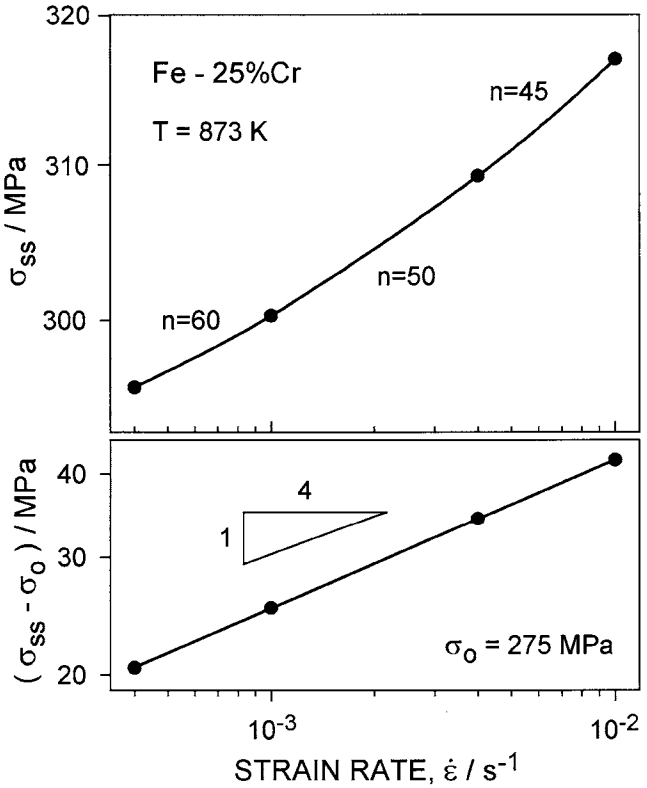

Fig. 2—Relationships between steady-state flow stress (σ_{ss}) and strain rate ($\dot{\varepsilon}$) in log-log scale for Fe-25 pct Cr at 873 K.

Here, σ_{ss} is an average flow stress at strains of 0.3 to 0.35. It is noted in Figure 2 that there is no linear relationship between σ_{ss} and $\dot{\varepsilon}$ in log-log scale. The stress exponent (n) is very high and increases with decreasing σ_{ss}. This can result from the second-phase particles distributed inside grains as well as the temperature region of athermal flow. The role of dispersed particles in deformation sometimes can be discussed using so-called threshold stresses. Chaudhury and Mohamed[15] proposed a simple technique to evaluate the threshold stress by using the following equation:

$$n_a = n/(1 - \sigma_0/\sigma) \qquad [1]$$

where n_a and n are an apparent and a true stress exponent and σ_0 and σ are the threshold and applied stress, respectively. Substituting the experimental data in Eq. [1], n is 4 and σ_0 is 275 MPa. The relationship between log ($\sigma_{ss} - \sigma_0$) and log $\dot{\varepsilon}$ can be represented by a linear line with a slope of 4, as shown in Figure 2.

B. *Deformation Relief*

Slip patterns appearing during plastic deformation at 873 K and at 10^{-3} s^{-1} were observed in the parallel plane to the compression axis and are shown in Figure 3. In early stages of plastic flow ($\varepsilon = 0.1$), long parallel slip bands with a spacing of 4 to 10 μm dominate and very fine wavy bands appear between coarse slip bands (Figure 3(a)). In the vicinity of grain boundaries, the density of slip bands is higher than that in grain interiors. With further straining to 0.5, deformation microbands, as proved by Figures 4 and 6, are developed as crossing over the initial coarse slip bands (Figure 3(b)). These structures may be equivalent to the fragmented structure.[8] These microbands were more frequently evolved with increasing strain. The deformation relief appearing at high strains was investigated using the samples predeformed to 1.05, polished after unloading, and then redeformed to 1.15. The deformation relief in Figure 3(c) is quite different from those in Figures 3(a) and (b). It can be noted here that fine short slip lines appear and small isolated grains of about a few microns in size are evolved in these regions. This suggests that new grain formation followed by boundary sliding can take place at high strains.

C. *Deformation Microstructures*

The deformation microstructures developed at 873 K and 10^{-3} s^{-1}, corresponding to the deformation relief in Figure 3, are shown in Figure 4. The microbands mentioned previously are more frequently formed in the vicinity of initial grain boundaries, as shown in Figure 4(a). Compression to around a strain of 0.7 leads to the pancaking of the original grains and the formation of microbands, their clusters and/or their crossing within them. These clusters involve some microbands of a few microns in width and are inhomogeneously developed. It also can be seen in Figure 4(a) that original grain boundaries are serrated at the sites, where the deformation bands reach them. Further deformation leads to decreasing the spacing of microbands while increasing their width. The volume fraction of such regions, including microband clusters, becomes around 80 pct in the central part of deformed samples, while it becomes over 40 pct as a whole at a strain of 1.05 (Figure 4(b)). Small grains of about 1 μm in size can be recognized to be developed in these band interiors. As the deformation bands are more frequently evolved near the original grain boundaries, the latter cannot be exactly recognized in Figure 4(b).

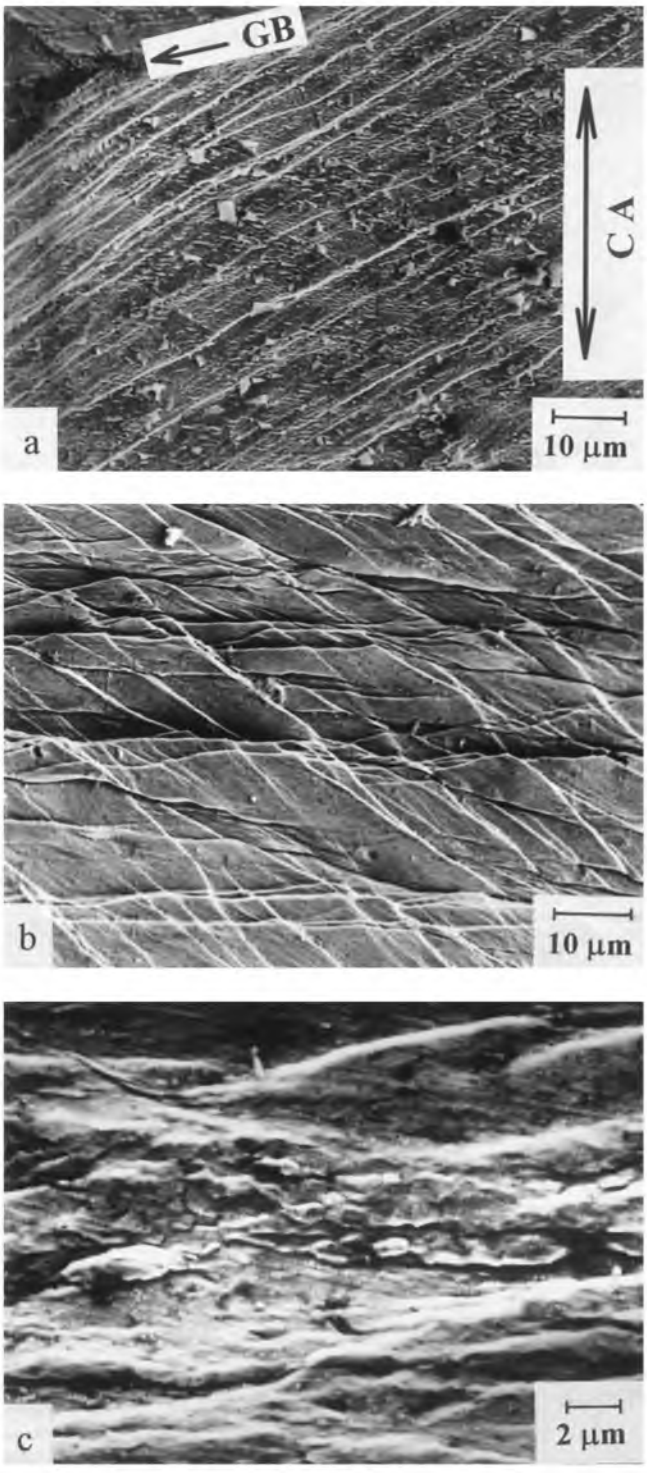

Fig. 3—Deformation relief for Fe-25 pct Cr deformed to various strains at 873 K and at 10^{-3} s^{-1}. CA indicates compression axis. The sample in (c) was deformed to $\varepsilon_{pre} = 1.05$, repolished after unloading, and then redeformed to $\varepsilon = 0.1$. (*a*) $\varepsilon = 0.1$, (*b*) $\varepsilon = 0.5$, and (*c*) $\varepsilon = 1.15$.

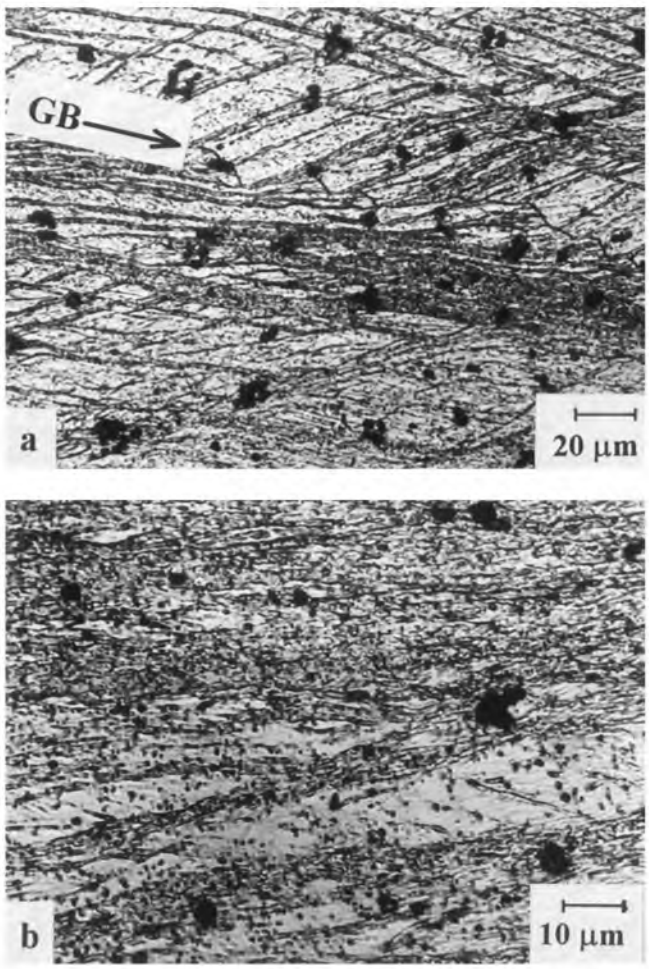

Fig. 4—Development of the clusters of microbands in Fe-25 pct Cr deformed at 873 K and at 10^{-3} s^{-1}. Note in (a) that many microbands are evolved near the serrated grain boundaries: (*a*) $\varepsilon = 0.7$ and (*b*) $\varepsilon = 1.05$.

Some typical TEM microstructures for the same samples in Figures 3 and 4 are shown in Figure 5. Long DDWs parallel to one another are formed at early stages of deformation (Figure 5(a)). The dislocation densities between DDWs are around 5×10^{14} m^{-2}. The average misorientation of neighboring microregions subdivided by DDW is 0.5 to 1 deg and the maximum value is about 2 deg. On the other hand, fragmented structures are formed in the form of chains of elongated fragments in the vicinity of initial grain boundaries, as shown in Figure 5(b). The size of fragments is about 1.1 μm in the longitudinal direction and 0.6 μm in the transverse one. It should be noted in Figure 5(b) that the misorientations of longitudinal boundaries are clearly higher than those of transversal ones. It can be stressed here that mutual misorientations of longitudinal fragmented boundaries are almost counteracting, *i.e.*, for example, $\theta_{AB} = 7$ deg and $\theta_{BC} = 24.5$ deg, while $\theta_{AC} = 19.4$ deg (Figure 5(b)). The true misorientation between A and C (θ_{AC}) is nearly equal to the value of $\|\theta_{AB}| - |\theta_{BC}\| = 17.5$ deg. The fragmented areas are surrounded by high-angle boundaries, which may be called geometrically necessary boundaries.[14] When such dislocation boundaries intersect the initial grain boundaries, the latter can locally migrate assisted by dynamic recovery and then change to irregular shapes as their angles become about 120 deg at triple junctions (Figure 5(b)). It should be noted that very fine particles, such as titanium and chromium carbides, precipitate in dislocation boundaries. Their average size was about 20 nm and their volume fraction did not exceed 0.5 pct.

Upon further straining to 0.7 (Figure 6), the DDWs became narrower and the dislocations inside the DDWs could

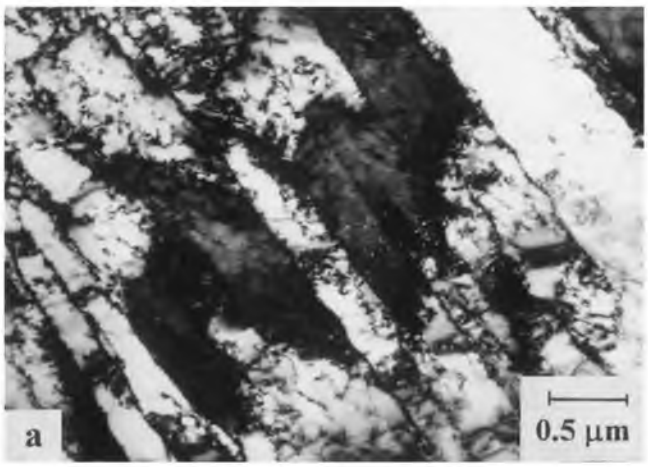

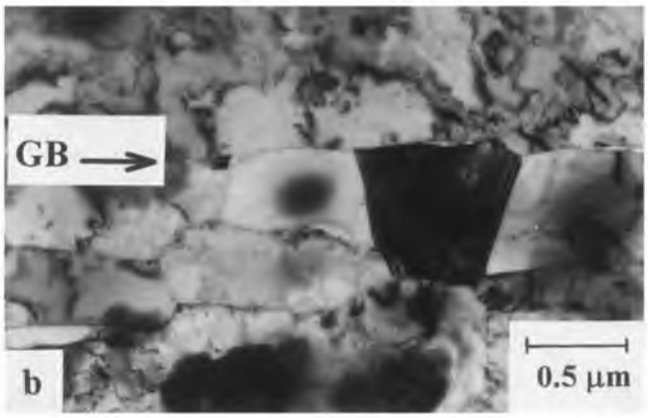

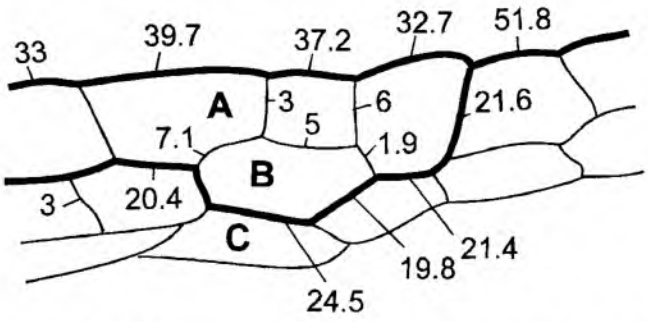

Fig. 5—Typical TEM microstructures evolved in Fe-25 pct Cr deformed to $\varepsilon = 0.15$ at 873 K and under 10^{-3} s^{-1}. (*a*) Dense dislocation walls and (*b*) fragmented structure near a grain boundary.

not be distinguished, while the dislocation densities developed between DDWs did not roughly change with strain. It is remarkable in Figure 6 that several deformation microbands are evolved by intersecting the DDWs. The misorientations between such microbands and the matrices composed of DDWs did not exceed 4 deg. With an increase in strain, many microbands were developed as crossing original grain interiors, followed by the evolution of their clusters, and finally the so-called fragmented structures inside these clusters, as represented in Figure 7. Here, note the misorientations between adjacent fragments, *e.g.*, *A*, *B*, *C*, *D*, and *E*, in Figure 7(a). The results of $\theta_{AC} = 1.8$ deg, $\theta_{AD} = 7.2$ deg, and $\theta_{AE} = 21.8$ deg suggest that the misorientations of these fragmented boundaries are compensated, as mentioned previously. The width of the fragmented bands and the boundary misorientations increase with further deformation to $\varepsilon = 1.05$ (Figure 7(b)). It can be clearly recognized in Figure 7(b) that new fine grains with medium to high angle boundaries are completely developed in the fragmented structure and become more equiaxed, accompanied by increases in their boundary misorientations and decreases in internal dislocation densities. The average grain size is 1.1 ± 0.2 μm in Figure 7(b).

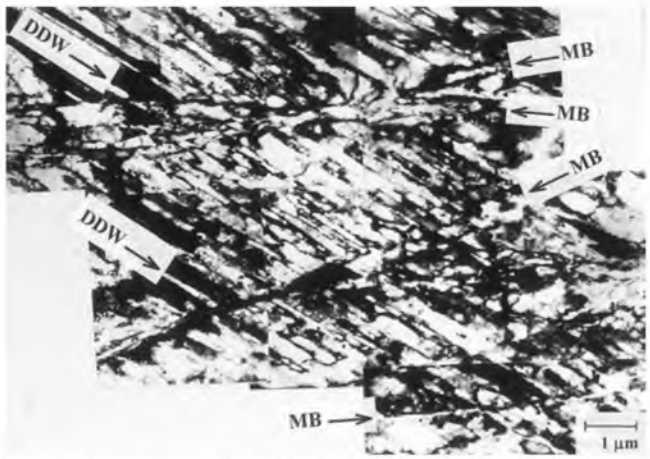

Fig. 6—Some microbands developed as crossing DDWs in Fe-25 pct Cr deformed to a moderate strain ($\varepsilon = 0.7$) at 873 K and at 10^{-3} s^{-1}.

Figure 8 shows the changes in the distribution of boundary misorientations in the fragmented structure with deformation at 873 K and at 10^{-3} s^{-1}. It is evident in Figure 8 that the fragmented structure is composed of dislocation boundaries with low to middle angles at $\varepsilon = 0.7$, while the boundaries have mostly high angles at $\varepsilon = 1.05$. Specifically, the fraction of high-angle boundaries increases substantially with strain. The fragmented interiors had relatively lower dislocation densities (5×10^{13} m^{-2}) as compared with the regions between DDWs (around 5×10^{14} m^{-2}).

The changes in X-ray physical line broadening (β) and microstrain ($\Delta d/d$) in the deformed matrices with warm deformation are shown in Figure 9. The broadening derived from a plane of [220] increases and maximizes as strain increases up to around 0.7 and then decreases at higher strains. The ratio of $\beta_{[220]}/\beta_{[110]}$ is close to the value of tan $\theta_{[220]}$/tan $\theta_{[110]}$ within the experimental accuracy, where $\theta_{[hkl]}$ is the X-ray diffraction angle. According to the assumption that the broadening can be caused by microdistortion, it is possible to estimate an amount of internal elastic stress (σ) by the following equation[16]

$$\sigma = \beta_{[hkl]}\, G/4 \tan \theta_{[hkl]} \qquad [2]$$

where G is the shear modulus. Using the data in Figure 9 and Eq. [2], internal stresses evolved can decrease from about 5×10^{-4} G at $\varepsilon = 0.7$ to 3×10^{-4} G at $\varepsilon = 1.05$ accompanied with the development of equiaxial new grains.

IV. DISCUSSION

It has been clarified from the present work that microstructures evolved during warm deformation are characterized by the formation of DDWs at low strains, microbands and their clusters at moderate strains, and finally new fine

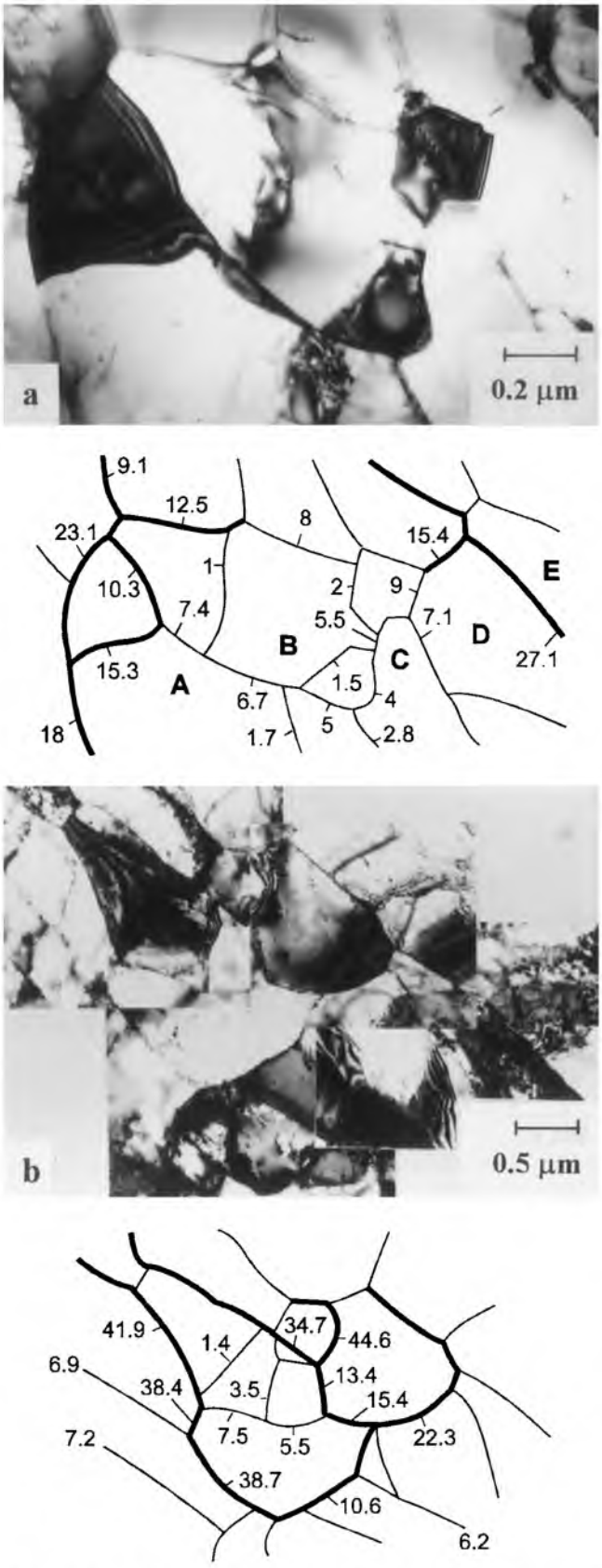

Fig. 7—Typical fragmented structures evolved inside the clusters of microbands of Fe-25 pct Cr deformed at 873 K and at 10^{-3} s^{-1}. Thin and thick lines indicate low- and high-angle boundaries, respectively. (*a*) ε = 0.7 and (*b*) ε = 1.05.

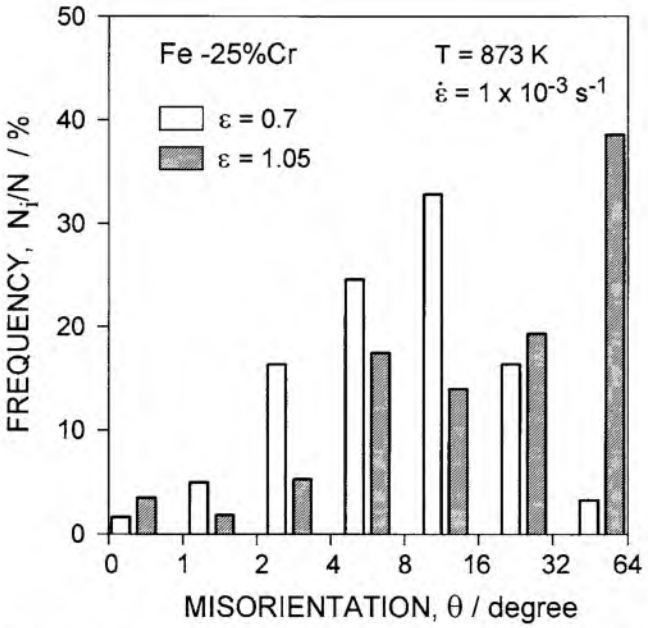

Fig. 8—Dislocation boundary misorientations distributed in the fragmented structures evolved in Fe-25 pct Cr deformed to ε = 0.7 and ε = 1.05 at 873 K and at 10^{-3} s^{-1}.

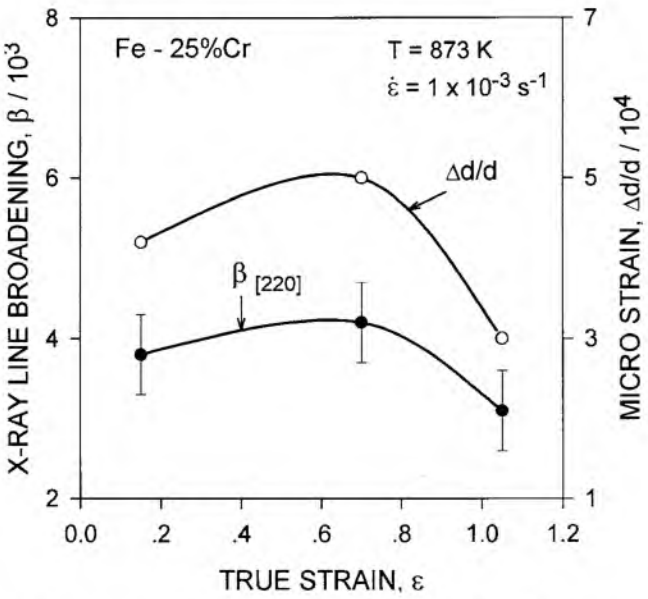

Fig. 9—Changes in X-ray line broadening (β) and lattice microstrain ($\Delta d/d$) with strain for Fe-25 pct Cr deformed at 873 K and at 10^{-3} s^{-1}.

grains inside the latter at higher strains. The kinetics of such microstructure evolution can be affected by the mechanisms operating during warm deformation. The understanding of the inter-relation between the deformation mechanisms and structure formation mechanisms, therefore, is of particular importance, because only this approach can allow a non-contradictory explanation for the structure evolution taking place in materials with complex strain behavior.[1–7,10,13,14]

At an early stage of deformation, slip takes place homogeneously, leading to increasing dislocation densities and then to a localization of plastic deformation on a microscale level (*i.e.*, size of DDWs). The strain hardening taking place at low strains results from the increase of dis-

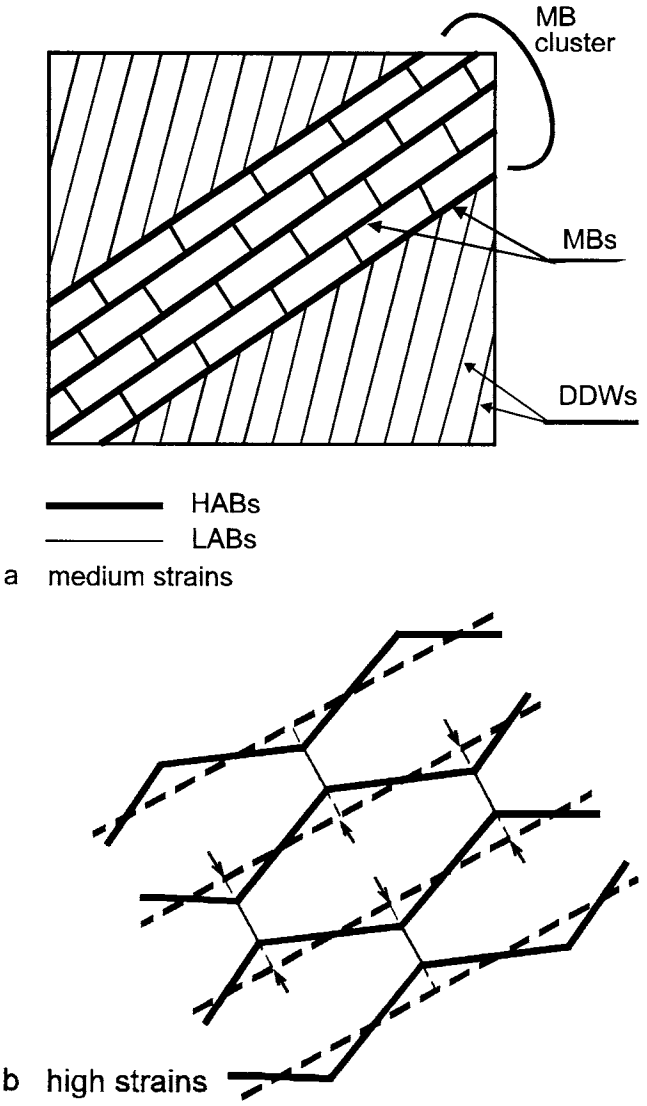

Fig. 10—Schematic drawing of fine grain formation during warm deformation. (*a*) Fragmented structure developed inside microband clusters at medium strains. (*b*) New fine grain formation accompanied by local migration of fragmented boundaries and dynamic recovery at high strains. Bold and thin lines indicate high- and low-angle boundaries, respectively. Chain lines show earlier boundary positions.

location density followed generally by the formation of the DDWs.[4,8,9,11,12,14] In this case, the average dislocation densities can be related to the applied stress. They approach a saturation value with warm deformation, and then the deformation processes should be changed because of deformation instability, *i.e.*, strain localization taking place on a mesoscopic scale (*i.e.*, size of microbands).[4,14,17] The microbands are generally evolved as intersecting DDW (Figure 6) and progressively evolved with strain, leading to the formation of microband clusters in the pancaked grain interiors at high strains. The dislocations evolved inside such microband clusters should be rearranged by dynamic recovery, including dislocation climbing, finally followed by the formation of the fragmented structure (Figures 5(b) and 7). It should be noted that the longitudinal boundaries of fragmented structure are parallel to those of the previous microbands. The formation of such fragmented structure can bring about the decreases in strain hardening and finally the appearance of apparent steady-state flow at high strains.

Let us consider here the effect of microband clusters on the deformation behavior of Fe-25 pct Cr alloy by using the modern concept of deformation-induced high-angle boundaries (HABs).[17,18] The fact that the evolution of dislocation assemblage leads to the formation of HABs has been explained by the collective modes of dislocation motion.[17] According to this model, microband formation can result from the evolution of dipoles of partial disclinations and their motion in grain interiors. The flow stresses at moderate strains can be explained as a result of the interaction between moving dipoles of partial disclinations and pre-existing DDWs. The critical stress for this interaction is represented by Eq. [3].[17]

$$\sigma = G\omega/(4\pi\,(1 - \nu)) \qquad [3]$$

where ω is the maximal misorientation in DDW and ν is the Poisson ratio. When $\omega = 0.04$ in the present results, σ is 230 MPa. The difference between the threshold stresses of 275 MPa (Figure 2) and 230 MPa can be explained by particle hardening due to some carbide precipitates.

At moderate strains, say, $\varepsilon = 0.7$, the dislocation densities evolved between DDWs hardly increase irrespective of the increase in internal stress (Figure 9). The microbands and their clusters are progressively developed with an increase in strain, finally followed by the formation of fragmented structures. The new boundaries in the latter, composed of the disclination-type defects, can be nonequilibrium and so cause long-range stress fields to increase.[17,19] The latter result from nonequilibrium boundaries can be estimated by using Nazarov's model:[19]

$$\sigma \approx 0.14G\mathbf{b}_{BD}/((1 - \nu)\sqrt{hx}) \qquad [4]$$

where $\mathbf{b}_{BD}$ is the Burgers vector of boundary dislocation with the space of h and x is the distance from the boundary plane. The average of h here is assumed to be $h \approx 9\,\mathbf{b}_{BD}$,[19] and $\mathbf{b}_{BD} = 1/6[111]$ as a general Burgers vector of partial dislocations in bcc lattice.[20] Then, at a distance $x = 0.65$ μm from the boundary plane, which is of order of fragmented size, σ is $7 \times 10^{-4}\,G$. Thus, the dislocation boundaries in fragmented structure may become the sources of internal stress fields. It can be concluded from the discussions that the dislocation densities developed in fragmented structures should be decreased by the operation of dynamic recovery, while the internal stresses based on the dislocation boundaries increase.

Finally, the processes of new grain formation during warm deformation will be discussed. The movement of disclination dipoles gives rise to the evolution of boundaries having opposite misorientations. This is supported by the results in Figures 5(b) and 7(a) namely, that the boundary misorientations in fragmented structures are mutually compensated. Fragmented structures are first formed near the initial grain boundaries, which are the preferential sites of disclination nucleation [18]. Upon further straining, such disclination dipoles become far away and then the microbands are formed as intersecting the grain interiors. Dynamic recovery takes place favorably in the regions composed of closely spaced microbands and their clusters, followed by the development of a fragmented structure (Figure 10(a)). The dislocation boundary misorientations in

fragmented structures increase with further deformation, leading to the evolution of HABs accompanied with their local migration. Dislocation climb as well as boundary sliding taking place along fragmented boundaries can bring about the development of HABs and so the relaxation of internal stresses. The energy balance between these boundaries can cause an equilibrium shape of triple junctions promoting local migration of the boundaries, as shown by the arrows in Figure 10(b). Finally, new equiaxed grains with HABs are developed in the matrix including DDWs at high strains, leading to the drop of internal stresses.

It can be concluded from the discussions described previously that the processes of new grain formation during warm deformation of a ferritic steel cannot be explained only by simple polygonized processes. The operation of localized deformation can lead to the formation of microbands and their clusters as well as the fragmented structure accompanied with the formation of HABs. The misorientation of such dislocation boundaries in the fragmented structure changes from low to high angle, and these boundaries, assisted by dynamic recovery, become corrugated. Finally, new equiaxed grains with low to high angle misorientations are fully developed in the matrices, including homogeneous DDWs. This phenomenon looks like a kind of continuous dynamic recrystallization and can be called an apparent dynamic recrystallization.

V. CONCLUSIONS

The plastic deformation and the development of new fine grains in a ferritic steel with high SFE were studied in compression at a moderate temperature (0.5 T_m), and the main results obtained can be summarized as follows.

1. Flow stresses at strains of beyond 0.25 hardly depend on strain and strain rate because of the athermal region of deformation at around 0.5 T_m. This is an apparent steady-state flow because heterogeneous deformation frequently takes place during straining.
2. The substructure development accompanied with deformation includes the formation of DDWs and microbands and their clusters, followed by the evolution of fragmented structure inside microbands.
3. The misorientations of the dislocation boundaries in the fragmented structure change from low to high angle with deformation, and these boundaries move locally, assisted by dynamic recovery, leading to the formation of corrugated shape.
4. New equiaxed grains with low to high angle misorientations are fully developed in the clusters of MBs. The process of such dynamic formation of new grains can be called an apparent dynamic recrystallization.

ACKNOWLEDGMENTS

The authors are grateful to the Ministry of Education of Japan for financial support under a grant for scientific research. One of the authors (AB) thanks the Japan Society for the Promotion of Science and the University of Electro-Communications for providing scientific fellowships.

REFERENCES

1. T. Sakai and J.J. Jonas: *Acta Metall.*, 1984, vol. 32, pp. 189-209.
2. T. Sakai: *J. Mater. Processing Technol.*, 1995, vol. 53, pp. 349-61.
3. H.J. McQueen and J.J. Jonas: *J. Appl. Met.*, 1984, vol. 3, pp. 233-41.
4. A.N. Belyakov and R.O. Kaibyshev: *Phys. Met. Metallogr.*, 1993, vol. 76, pp. 162-67.
5. R. Kaibyshev and O. Sitdikov: *Z. Metallkd.*, 1994, vol. 85, pp. 738-43.
6. M. Furukawa, Z. Horita, M. Nemoto, R.Z. Valiev, and T.G. Langdon: *Acta Mater.*, 1996, vol. 44, pp. 4619-29.
7. G.A. Salishchev, R.G. Zaripova, A.A. Zakirova, and H.J. McQueen: *Hot Workability of Steels and Light Alloys-Composites*, H.J. McQueen, E.V. Konopleva, and N.D. Ryan, eds. TMS-CIM, Montreal, 1996, pp. 217-26.
8. A.N. Vergazov, V.A. Likhachev, and V.V. Rybin: *Phys. Met. Metallogr.*, 1976, vol. 42, pp. 101-06.
9. S. Dymek and M. Blicharski: *Z. Metallkd.*, 1985, vol. 76, pp. 777-85.
10. A. Korbel, J. Rys, and M. Szczerba: *Acta Metall.*, 1985, vol. 33, pp. 2215-19.
11. N. Hansen: *Metall. Trans. A*, 1985, vol. 16A, pp. 2167-90.
12. B. Bay, N. Hansen, D.A. Hughes, and D. Kuhlmann-Wilsdorf: *Acta Metall. Mater.*, 1992, vol. 40, pp. 205-19.
13. W. Bochniak and M. Niewczas: *Z. Metallkd.*, 1993, vol. 84, pp. 211-15.
14. D.A. Hughes, Q. Liu, D.C. Chrzan, and N. Hansen: *Acta Mater.*, 1997, vol. 45, pp. 105-12.
15. P.K. Chaudhury and F.A. Mohamed: *Acta Metall.*, 1988, vol. 36, pp. 1099-1110.
16. K.W. Andrews: *Physical Metallurgy. Techniques and Applications*, George Allen & Unwin Ltd., London, 1973, vol. 1, pp. 252-61.
17. V.I. Vladimirov and A.E. Romanov: *Disklinatsii v Kristallakh (Disclinations in Crystals)*, Nauka, Leningrad, Russia, 1986, pp. 181-90.
18. V.V. Rybin, A.A. Zisman, and N.Yu. Zolotorevsky: *Acta Metall. Mater.*, 1993, vol. 41, pp. 2211-17.
19. A.A. Nazarov, A.E. Romanov, and R.Z. Valiev: *Acta Metall. Mater.*, 1993, vol. 41, pp. 1033-40.
20. J.P. Hirth and J. Lothe: *Theory of Dislocations*, Krieger Publishing Company, Malabar, FL, 1992, pp. 366-73.